Journal of Analytical and Applied Pyrolysis 113 (2015) 508–517

Contents lists available at ScienceDirect

Journal of Analytical and Applied Pyrolysis

journal homepage: www.elsevier.com/locate/jaap

Copyrolysis of peanut shells and cassava starch mixtures: Effect of the components proportion

L.I. Gurevich Messina[a,b], P.R. Bonelli[a,b], A.L. Cukierman[a,b,c,*]

[a] Programa de Investigación y Desarrollo de Fuentes Alternativas de Materias Primas y Energía – PINMATE, Departamento de Industrias, Facultad de Ciencias Exactas y Naturales, Universidad de Buenos Aires, Ciudad Universitaria, Intendente Güiraldes 2620, C1428BGA Buenos Aires, Argentina
[b] Consejo Nacional de Investigaciones Científicas y Técnicas (CONICET), Av. Rivadavia 1917, C1033AAJ Buenos Aires, Argentina
[c] Cátedra de Tecnología Farmacéutica II, Departamento de Tecnología Farmacéutica, Facultad de Farmacia y Bioquímica, Universidad de Buenos Aires, Junín 956, C1113AAD Buenos Aires, Argentina

ARTICLE INFO

Article history:
Received 20 October 2014
Received in revised form 26 March 2015
Accepted 28 March 2015
Available online 30 March 2015

Keywords:
Copyrolysis
Peanut shells
Cassava starch
Waste management

ABSTRACT

Copyrolysis of peanut (*Arachis hypogaea*) shells and cassava (*Manihot esculenta*) starch using mixtures of different proportions was examined to improve yield of the bio-oil and its quality. Pyrolysis of the individual components was also investigated in order to quantify the improvement of the measured properties. The kinetics of pyrolysis/copyrolysis was characterized by thermogravimetrical analysis and the application of two different models: one which takes into account the deactivation of the solid, and another one which assumes a normal distribution of the activation energy. Interactions between the starch and the shells were inferred since maximum reaction rates were, in all cases, lower than the weighed average values obtained for the pyrolysis of the individual components. Furthermore, both the bio-oil yield and the water content of the liquids showed synergistic effects. A mixture composed by 75 wt% of starch and 25 wt% of peanut shells led to maximize the yield of the bio-oil (58.2 wt%), while its water content was reduced in 3.4% in comparison with the value expected from the weighed average of the individual results. On the other hand, the addition of the starch to the peanut shells led to a bio-char with less ash content. It could be more suitable for further combustion in steam boilers.

1. Introduction

The abundant lignocellulosic by-products generated in the industrialization of agricultural, agro-industrial, forest and/or food products, generically known as biomass, represent alternative renewable resources which are potentially attractive to produce bio-energy and chemical products, especially in countries whose economies are heavily based on activities related to the agro-industry [1,2]. Biomass shows advantages compared to conventional fossil fuels, such as lower sulfur and heavy metal contents, high availability, and renewable nature. Furthermore, the use of biomass as a fuel or as raw material to produce fuels is neutral from the viewpoint of greenhouse gas emission since the CO_2 released in combustion is balanced by the CO_2 captured by the plants during their growth [3]. These facts and the limited coal and oil reserves have led to study biomass conversion to bio-energy toward a gradual replacement of fossil fuels. This substitution may also contribute to the global strategy of reducing environmental pollution [4,5].

Bio-energy generation via thermochemical conversion has advantages in comparison to the biochemical route, such as higher reaction rates and superior capacity to destroy organic matter [6]. Among thermochemical processes, pyrolysis, namely the thermal degradation of biomass in an inert atmosphere, is particularly interesting because of the huge range of resulting products [7]. Among them, the liquid products, known as bio-oils, are of great interest because of their potential as bio-fuels. They share the advantages of many other liquid fuels, such as a low transport cost, high energetic density, and the feasibility of being employed in combined cycle gas turbine to generate electricity [8]. However, the high water content of the bio-oils and the large amount of oxygenated compounds cause difficulties for their direct combustion [9].

Several efforts have been made in order to improve the quality of the bio-oils. Zeolite cracking and hydrodeoxygenation have been two of the most studied catalytic processes for their

* Corresponding author at: Programa de Investigación y Desarrollo de Fuentes Alternativas de Materias Primas y Energía – PINMATE, Departamento de Industrias, Facultad de Ciencias Exactas y Naturales, Universidad de Buenos Aires, Ciudad Universitaria, Intendente Güiraldes 2620, C1428BGA Buenos Aires, Argentina.
Tel.: +54 11 45763383; fax: +54 11 45763366.
E-mail address: analea@di.fcen.uba.ar (A.L. Cukierman).

http://dx.doi.org/10.1016/j.jaap.2015.03.017
0165-2370/

upgrading [7]. However, in spite of reducing the oxygen content of the fuel, both processes require expensive catalysts. Zeolite cracking generates even more water, which could reduce combustion temperature. Also, the large amount of produced coke may promote the deactivation of the catalysts. On the other hand, hydrodeoxygenation needs high hydrogen pressures and, therefore, the equipment becomes high-priced [10–12].

Compared to these approaches, pyrolysis of mixtures of biomass and biopolymers (copyrolysis) could be an economical way to improve bio-oils' quality even though it has been scarcely examined. A recent work by Cornelissen et al. [13] has shown that the addition of potato starch to willow wood and its subsequent thermal degradation lead to an increase in bio-oil production and a reduction in its water content. However, the copyrolysis of maize starch and the same lignocellulosic material did not improve the bio-oil yield neither its water content. Therefore, the starch source would influence the resulting products. To the best of our knowledge, almost no other work has been devoted to examine the copyrolysis of starch with lignocellulosic biomaterials. Moreover, the aforementioned work did not study the characteristics of the generated bio-chars and pyrolysis gases which play an important role in the process sustainability [14].

Within this scenario, in the present work copyrolysis of the starch from cassava (*Manihot esculenta*) and peanut *(Arachis hypogaea)* shells was investigated. Cassava is a tuber with a high content of starch largely cultivated in South America. Annual production of cassava was estimated at approximately 29 Mt in 2013 for the whole continent [15,16]. The processing of the tubers to obtain the starch generates a bagasse that constitutes 15–20%, in weight, of the cassava tuber. This waste contains around 50–70% of starch on a dry basis [17]. In this study, cassava starch was used as a representative of the dry bagasse. Likewise, Argentina is one of the largest producers of peanut in the world with an estimated production of over 1 Mt in 2013 [16,18]. Its industrial processing generates abundant shells that represent about one fourth of the peanut fruits weight and have great potential to be converted into energy [19,20].

In order to examine the behavior of the thermal degradation of the starch waste while being pyrolyzed along with the peanut shells, three mixtures of different weight proportions (75 wt%, 50 wt%, 25 wt%) were prepared. Thermogravimetry was applied to investigate the kinetics of the pyrolysis and copyrolysis processes. The experimental results were then represented by two models which take into account variations of the process activation energy, the deactivation model and the distributed activation energy model (DAEM). To gain insight into interactions between the starch and the peanut shells, thermogravimetric experiments using mixtures of equal proportions of the starch and each of the main lignocellulosic biopolymers constituents of the shells, i.e., cellulose, hemicellulose, and lignin, were further carried out. Besides, the peanut shells, the cassava starch, and their mixtures were separately pyrolyzed in a fixed bed reactor at pre-established conditions. Yields of the three kinds of pyrolysis products and their physicochemical properties were determined.

2. Materials and methods

2.1. Materials

Commercial peanut *(A. hypogaea)* shells, labeled as PS100, were used. They were cleaned, milled, and screen-sieved. Fractions of particle diameter between 250 μm and 500 μm were reserved for the reactor assays, while samples with a particle diameter between 44 μm and 74 μm were selected for thermogravimetric studies.

Cassava (*M. esculenta*) starch, designated ST, was provided by Bernesa S.A. In order to use the same particle diameter of the peanut shells samples, the cassava starch powder was processed by wet granulation [21], and then milled and screen-sieved. Three samples of different proportions of the biomass and the biopolymer were prepared by physical mixing: 75 wt% shells–25 wt% starch (PS75); 50 wt% shells–50 wt% starch (PS50); 25 wt% shells–75 wt% starch (PS25).

Microcrystalline cellulose, purchased from Droguería Saporiti, xylan, provided by Sigma–Aldrich®, and lignin extracted from the peanut shells, as described below (Section 2.2), were employed to investigate possible synergistic effects between the cassava starch and these biopolymers. For this purpose, the starch powder was mixed in equal proportions with each of the three lignocellulosic biopolymers. Xylan was used as a model compound representative of hemicellulose [22].

2.2. Biomass and biopolymer characterization

Proximate analysis of the peanut shells and cassava starch samples was performed by thermogravimetric analysis (TA Instruments SDT Q600), according to American Society of Testing and Materials (ASTM) standards 5142. An automatic elemental analyzer (Carlo Erba model EA 1108) was used to determine their elemental composition.

To assess the content of main biopolymeric constituents, the Van Soest analysis was carried out. In this analysis, biomass is separated progressively into neutral detergent fiber (NDF), acid detergent fiber (ADF), and strong acid detergent fiber (SADF). NDF mainly consists of cellulose, hemi-cellulose, lignin and ash, while ADF is composed of cellulose, lignin and ash. Only lignin and ash are present in SADF [23]. On the other hand, amylose content of the cassava starch was analyzed by standardized iodine colorimetry, according to ISO 6647-2:2007. The absorbance of the starch–iodine mixture was measured at 620 nm. Amylopectin content was determined by difference.

In addition, the functional groups of both the shells and the starch were studied by Fourier transform infrared (FT-IR) spectroscopy. The spectra were recorded using a PerkinElmer IR Spectrum BXII spectrometer within the range 600–4000 cm^{-1}. Each sample was ground with KBr at an approximate ratio of 1:200 and the resulting mixture was then pressed. The background obtained from a scan of pure KBr was automatically subtracted from the sample spectra.

2.3. Thermogravimetric assays

Kinetic measurements for the pyrolysis of peanut shells, cassava starch, and their mixtures in different proportions were performed in a simultaneous thermal analyzer (TG–DSC/DTA TA Instruments SDT Q600) equipped with a N_2 flow device and a data acquisition system. Each sample was thermally treated under flowing N_2 from ambient temperature up to 500 °C. Experiments were carried out for samples' masses of 10 mg, fractions of 44–74 μm particle diameter, and heating rate of 10 °C/min. For these conditions, negligible diffusional effects were thoroughly verified from preliminary experiments. The same assays were performed in order to investigate possible synergy between the starch and the other biopolymers (hemicellulose, cellulose, and lignin).

2.4. Pyrolysis and copyrolysis in fixed bed reactor

To examine the influence of starch addition to peanut shells on yields and characteristics of the pyrolysis/copyrolysis products, experiments were conducted in a bench-scale fixed bed reactor. The equipment mainly consisted of a stainless steel (AISI 316)

fixed bed reactor (2.5 cm I.D., 110 cm total length) and an upper zone where the sample was stored before reaction started. The reactor was externally heated by an electrical furnace driven by a Yokogawa UT350 microprocessor based automatic controller. A chromel–alumel thermocouple was positioned at the geometrical center of the sample carrier. The sample was initially at ambient temperature. In order to start the pyrolysis/copyrolysis process, a valve, which connected the upper zone with the reactor, was opened and the thermocouple and the sample carrier were pushed until they were positioned in the reaction zone. At the reactor outlet, a series of flasks immersed in a cooling bath, using isopropyl alcohol at −10 °C as solvent, enabled condensation and collection of the condensable volatiles generated with the thermal degradation course.

From preliminary experiments, it was found that the temperature of the process was the variable that had the greatest influence on the bio-oil yield, being $T = 500\,^{\circ}C$ the temperature at which the pyrolysis of peanut shells led to a maximum yield of liquids. Also, it was determined that after 30 min the volatiles generation was negligible, indicating almost complete conversion. Other conditions, such as the particle diameter or the inert gas flow rate, had a weak influence on the process. Therefore, the following pre-established operating conditions were chosen: $T = 500\,^{\circ}C$, N_2 flow rate = 300 mL min^{-1}, particle diameter = 250–500 μm; samples' masses = 10–15 g, holding time = 30 min.

The residual solid and the accumulated liquid products contained in the flasks were weighed to determine product yields. These products were then carefully stored in closed containers for further characterization. Percent yields were calculated as weight of product per total weight of raw sample. Gas yields were obtained by difference from overall mass balances.

2.5. Characterization of the pyrolysis products

Water content of the liquid samples was measured by volumetric Karl-Fischer titration (Methrom Herisau Karl Fisher Automat E 547) following ASTM E 203. The samples' pH was determined with an Orion 290A portable pH meter. Dichloromethane was used to extract the organic phase from the bio-oils (volume ratio solvent/bio-oil: 2:1). Elemental composition of the organic phase of the bio-oils and of the bio-chars was determined by ultimate analyses, as depicted above. Furthermore, their higher heating value (HHV) was also determined using a Parr 1341 oxygen bomb calorimeter.

Moreover, FT-IR analysis of the organic fractions of the bio-oils was carried out employing an attenuated total reflection (ATR) accessory made of SeZn in order to identify functional groups which are present in the bio-oils samples. The instrument already described in Section 2.2 was used. It automatically subtracts the background spectrum obtained from the SeZn crystal from the sample.

In addition, N_2 adsorption–desorption isotherms at −196 °C were determined for the bio-chars using an automatic Micromeritics ASAP-2020HV volumetric sorption analyzer. Prior to gas adsorption measurements, the samples were outgassed at 120 °C for two hours. Textural properties were assessed from the isotherms, according to conventional procedures depicted in detail in previous studies [24]. The Brunauer–Emmett–Teller (BET) surface area (S_{BET}) was determined by the standard BET procedure and total pore volumes (V_t) were estimated from the amount of nitrogen adsorbed at the relative pressure of 0.95 ($p/p_0 = 0.95$). Moreover, the bio-chars, as well as the raw materials, were examined by scanning electronic microscopy (SEM) in a Zeiss Supra 40 microscope equipped with a field emission gun. The samples were placed on an aluminum holder, supported on conductive carbon type, dried under vacuum, and sputter coated with Au–Pd.

Table 1
Characterization of peanut shells (PS100) and cassava starch (ST).

	PS100	ST
Proximate analysis [wt%]		
Moisture	6.5	11.8
Volatile matter	68.8	81.6
Ash	5.5	0.2
Fixed carbon[a]	19.2	6.4
Ultimate analysis [wt%, dry and ash-free basis]		
Carbon	49.6	44.4
Hydrogen	6.5	6.3
Nitrogen	1.8	0.1
Oxygen[a]	42.1	49.2
Biopolymer composition [wt%, dry and ash-free basis]		
Lignin[b]	30.9	–
Cellulose[b]	54.6	
Hemicellulose[b]	14.5	–
Amylose	–	22.9
Amylopectin[a]	–	77.1

[a] Estimated by difference.
[b] Ash-free NDF basis.

Non-condensable gases, after flowing through the condensation system, were sampled periodically using Teflon gas bags, and further analyzed with a Shimadzu GC-8 gas chromatograph supplied with a thermal conductivity detector and a concentric packed Altech CTR I column (6 ft × ¼ in). Argon as carrier gas and a temperature of 25 °C were employed.

All the experiments were performed at least three times. Differences between replicates were less than 5% in all cases. Average values are reported.

3. Results and discussion

3.1. Characterization of the raw materials

Chemical characteristics of both the peanut shells and the starch are shown in Table 1. Results from proximate and elemental analyses of the peanut shells as well as the contents of main biopolymeric constituents, i.e., cellulose, hemicellulose, and lignin, were similar to those reported in the literature [20,25]. Moreover, the amylose content of the starch, despite being slightly higher than the average, fell within the typical range of reported values [26].

FT-IR spectra for the peanut shells (PS100) and the cassava starch (ST) are comparatively illustrated in Fig. 1. Main differences between the spectra could be attributed to the lack or the presence of the functional groups characterizing lignin. The spectrum of PS100 presented peaks at 800–900 cm^{-1}, indicative of the out of plane bending of aromatic C—H bonds, at 1270 cm^{-1}, characteristic of the guaicyl aromatic ring vibration, and at around 1530 cm^{-1},

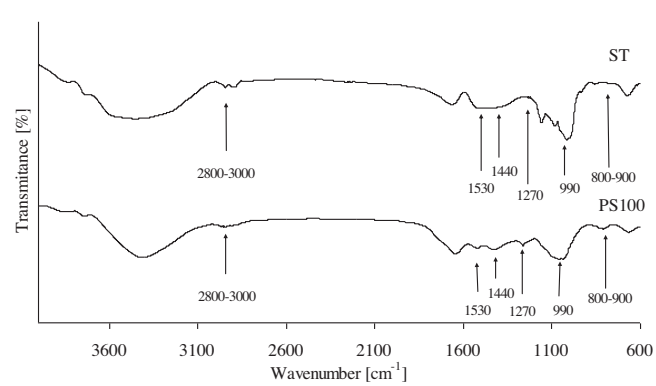

Fig. 1. Fourier-transform infrared (FT-IR) spectra for the cassava starch (ST) and the peanut shells (PS100).

assigned to aromatic skeletal vibration, that were not detected in the ST spectrum. In addition, PS100 spectrum showed a broader peak at the region from 2800–3000 cm^{-1}, characteristic of alkyl groups, than the one seen for ST. This would be due to the existence of *n*-propyl groups, which are part of the lignin, in the PS100 sample. On the other hand, both spectra shared the characteristic peaks of the polysaccharides, such as the one corresponding to the O—H in plane bending at 1440 cm^{-1} or the one typical of C—O valence vibration at 990 cm^{-1} [27,28].

3.2. Kinetic study of the pyrolysis/copyrolysis process

The effect of the starch content in the mixtures on the kinetics of the pyrolysis/copyrolysis processes was examined. Fig. 2a and b illustrate variations of the weight fractions (w) and pyrolysis rates ($-dw/dt$) with the temperature, respectively, for the five studied cases. The weight fractions were obtained as $w = m/m_0$, where m and m_0 are the dry mass of the sample at time t and the initial dry mass, respectively. As observed in Fig. 2a, thermal degradation of PS100 started at a lower temperature and took place more gradually than that for ST. Likewise, the thermal degradation of the lignocellulosic biomass ended at higher temperatures than the pyrolysis of the starch. The behavior may be attributed to the strong thermal resistance of lignin composing the shells to degrade in accordance with the aromatic nature of this biopolymer [29]. The peanut shells–starch mixtures showed intermediate behaviors between those characterizing the individual components. Furthermore, the pyrolysis of the mixtures with greater content of starch attained a lower residual weight fraction, indicating a higher conversion rate. As seen in Fig. 2b, increasing the starch content in the mixture enhanced the value of the maximum reaction rate. For both individual biomaterials, the maximum reaction rates occurred at almost the same temperature (310 °C). Other results for TGA/DTG experiments for peanut shells [28] and cassava starch [30], employing the same heating rate used in this work, also reported values of

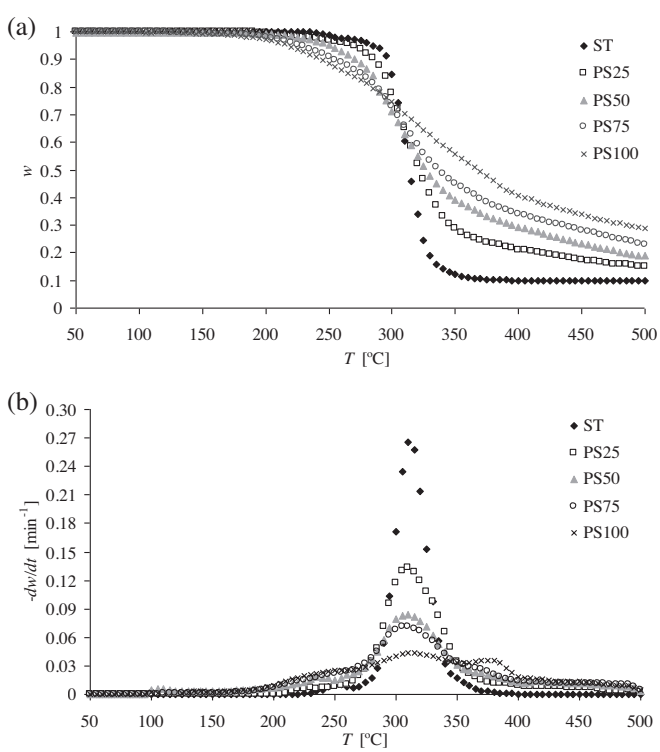

Fig. 2. TGA (a) and DTG (b) curves for the pyrolysis of cassava starch (ST) and peanut shells (PS100) and for the copyrolysis of their mixtures (PS25, PS50 and PS75).

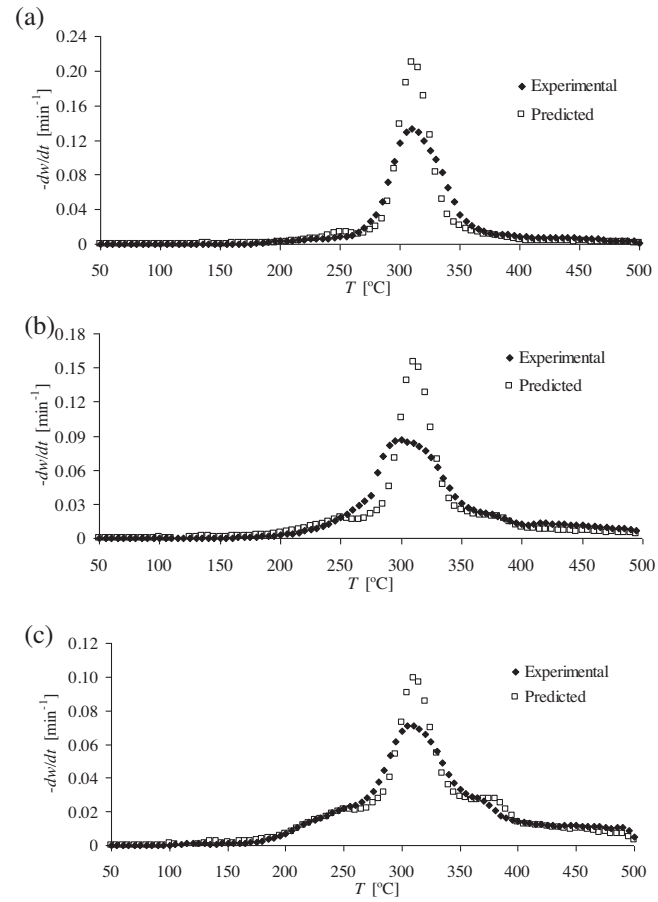

Fig. 3. Comparison between the experimental reaction rates of the copyrolysis of the different mixtures of cassava starch and peanut shells and values according to Eq. (1) calculated: (a) PS25, (b) PS50, and (c) PS75.

about 310 °C for the temperature where the peak took place. Interestingly, the mixture composition did not affect the temperature where the maximum reaction rate happened. It should be remarked that the similar values of temperatures for the maximum reaction rates do not mean that the pyrolytic behavior of PS100 and ST is analogous. As seen in Table 1, the biopolymer composition of ST and PS100 is very different and, therefore, differences in their thermal stability should be expectable. This will be further discussed in Section 3.3. On the other hand, the shoulder at 375 °C present in the DTG curve for PS100, which would correspond to the lignin decomposition, vanished with the increase of the starch content in the mixture.

In order to investigate possible interactions between the peanut shells and the cassava starch, the experimental values of the reaction rates of the three binary mixtures were compared with those calculated by addition of the reaction rate for each component multiplied by its proportion, as described by the following equation:

$$\left(-\frac{dw}{dt}\right)_{calc} = \left(-\frac{dw}{dt}\right)_{ST} m_{ST} + \left(-\frac{dw}{dt}\right)_{PS100} m_{PS100} \quad (1)$$

where ($-dw/dt$) is the reaction rate, and m, the weight fraction of the component in the mixture.

Comparisons between the experimental and calculated values for the copyrolysis of PS25, PS50 and PS75 are shown in Fig. 3a–c, respectively. In all the cases, the calculated value of the maximum reaction rate was higher than the experimental one, suggesting antagonistic effects. The interactions would be stronger for the pyrolysis of the PS50 mixture as the difference between the predicted and the experimental values was the highest, with the

former approximately duplicating the latter. These results will be further discussed in Section 3.3.

To represent the kinetics of the processes, modeling of the TGA curves was carried out. Two models were applied for this purpose: a deactivation model and the distributed activation energy model. The deactivation model considers that the activation energy increases with the reaction course. It is useful to fit the data when physico-chemical changes in the solid, such as alterations of its geometry and/or of the pore structure and volume shrinking, take place [31,32]. The model equations are given by:

$$-\frac{dw}{dt} = k_{ap}(w - w_\infty)^n \tag{2}$$

where n is the reaction order. For this study, $n = 1$ was considered since first order overall decompositions are generally used to describe the pyrolysis process [32]. Changes within the solid are assumed to affect the reaction rate constant, k_{ap}, and are taken into account through an increase of the activation energy with the temperature and the solid conversion according to:

$$k_{ap} = k_{0i} \exp\left[-\frac{E_{ai}\left(1 + \delta T z^\gamma\right)}{RT}\right] \tag{3}$$

where k_{0i} is the preexponential factor, E_{ai}, the initial activation energy, δ, the deactivation rate, and γ, the order with respect to the normalized fractional conversion. R and T are the universal gas constant and the absolute temperature, respectively. Besides, z in Eq. (3) represents the normalized fractional conversion which is defined as:

$$z = \frac{1 - w}{1 - w_\infty} \tag{4}$$

being w and w_∞ in Eq. (4) are the instantaneous and residual weight fractions, respectively.

The other applied model considers the thermal degradation as a set of parallel, first-order reactions. Instead of assuming a single value for the activation energy, it considers a Gaussian distribution $f(E)$. Moreover, this model assumes that the preexponential factor varies with the temperature [33]. The model equations are the following:

$$1 - w = \int_0^\infty \exp\left\{-\frac{A_0}{\beta}\left[\int_0^T T^{3/2} \exp\left(-E/RT\right) dT\right]\right\} f(E) dE \tag{5}$$

with the activation energy distribution being:

$$f(E) = \frac{1}{\sigma\sqrt{2\pi}} \exp\left[-\frac{(E - E_0)^2}{2\sigma^2}\right] \tag{6}$$

where E_0 is the mean value of distribution, and σ, the standard deviation. A_0 in Eq. (5) is a constant which affects the preexponential factor, and β, the heating rate. The other symbols are the same as in the deactivation model.

Both models were adjusted to the data minimizing the following objective function (O.F.):

$$\text{O.F.} = \sum \left(w_{exp} - w_{mod}\right)^2 \tag{7}$$

where w_{exp} and w_{mod} represent, respectively, the experimental data and the value predicted by the model.

The capability of each applied model to represent the experimental data is compared by estimating the standard deviation (s) as:

$$s = \sqrt{\frac{\sum \left(w_{exp} - w_{mod}\right)^2}{N - p}} \tag{8}$$

being N, the number of data, and p, the number of fitted parameters.

Model parameters are presented in Table 2. As seen, both models predicted an increment of the activation energy as greater the starch content of the mixture. Also, both models show rather higher values of standard deviation for the pyrolysis of ST samples. This could be due to the fact that the nth order kinetic models cannot fit accurately the sharp decrease in the instantaneous weight fraction for the pyrolysis of the starch [34].

The initial activation energy predicted for the pyrolysis of the cassava starch by the deactivation model (145 kJ mol^{-1}) is in agreement with the value reported by Marques et al. [30] (140 kJ mol^{-1}). On the other hand, it should be mentioned that activation energies reported in the literature for the pyrolysis of peanut shells present a wide range of values depending on the model and the experimental conditions applied. For instance, Zhang et al. [35] obtained a value of the activation energy of 84.5 kJ mol^{-1} for the pyrolysis of the peanut shells using the Friedman method, while Yuan et al. [28] predicted values of 253.9 kJ mol^{-1} and 244.3 kJ mol^{-1} applying the Flynn–Wall–Ozawa and the Kissinger–Akahira–Sunose methods, respectively.

The deactivation model parameters indicated that for the mixtures with greater starch content the activation energy of the process increased with the temperature more pronouncedly than for the pyrolysis of those with a high amount of peanut shells. As postulated by Balci et al. [36], the deactivation is more marked when the differences between the solid reactive and the solid product are more pronounced. In this sense, Fig. 4a–e shows SEM images of the biomaterials and the bio-chars generated in the fixed bed reactor. As seen in Fig. 4a and b, the PS100 sample and the generated bio-char shared a similar geometry. The former exhibited a fiber structure and the latter showed a partial linkage among the fibers. On the other hand, the particles of ST, having a spherical geometry, led to a bio-char mainly formed by large sheets (Fig. 4c and d). Thus, the deactivation would have been enhanced if the pyrolyzed material had been enriched with starch. The bio-char produced from the pyrolysis of PS50 mixtures exhibited an aspect

Table 2
Model parameters estimated for the pyrolysis of the peanut shells (PS100), the cassava starch (ST) and for the copyrolysis of their mixtures (PS25, PS50, PS75).

	PS100	PS75	PS50	PS25	ST
Deactivation model					
k_{0i} [min^{-1}]	1.0×10^4	2.9×10^4	1.8×10^6	8.9×10^7	8.9×10^{11}
E_{ai} [kJ mol^{-1}]	55	59	78	96	140
δ [K^{-1}]	3×10^{-4}	4×10^{-4}	5×10^{-4}	4×10^{-4}	1×10^{-3}
γ	2	4	5	8	200
s [%]	1.0	0.9	1.1	1.9	4.0
DAEM model					
A_0 [min^{-1}]	2.57	3.43	3.07	21.5	243
E_0 [kJ mol^{-1}]	62	63	62	72	78
σ [kJ mol^{-1}]	7.5	5.5	4.4	2.1	1.7
s [%]	0.6	1.8	2.7	3.7	6.4

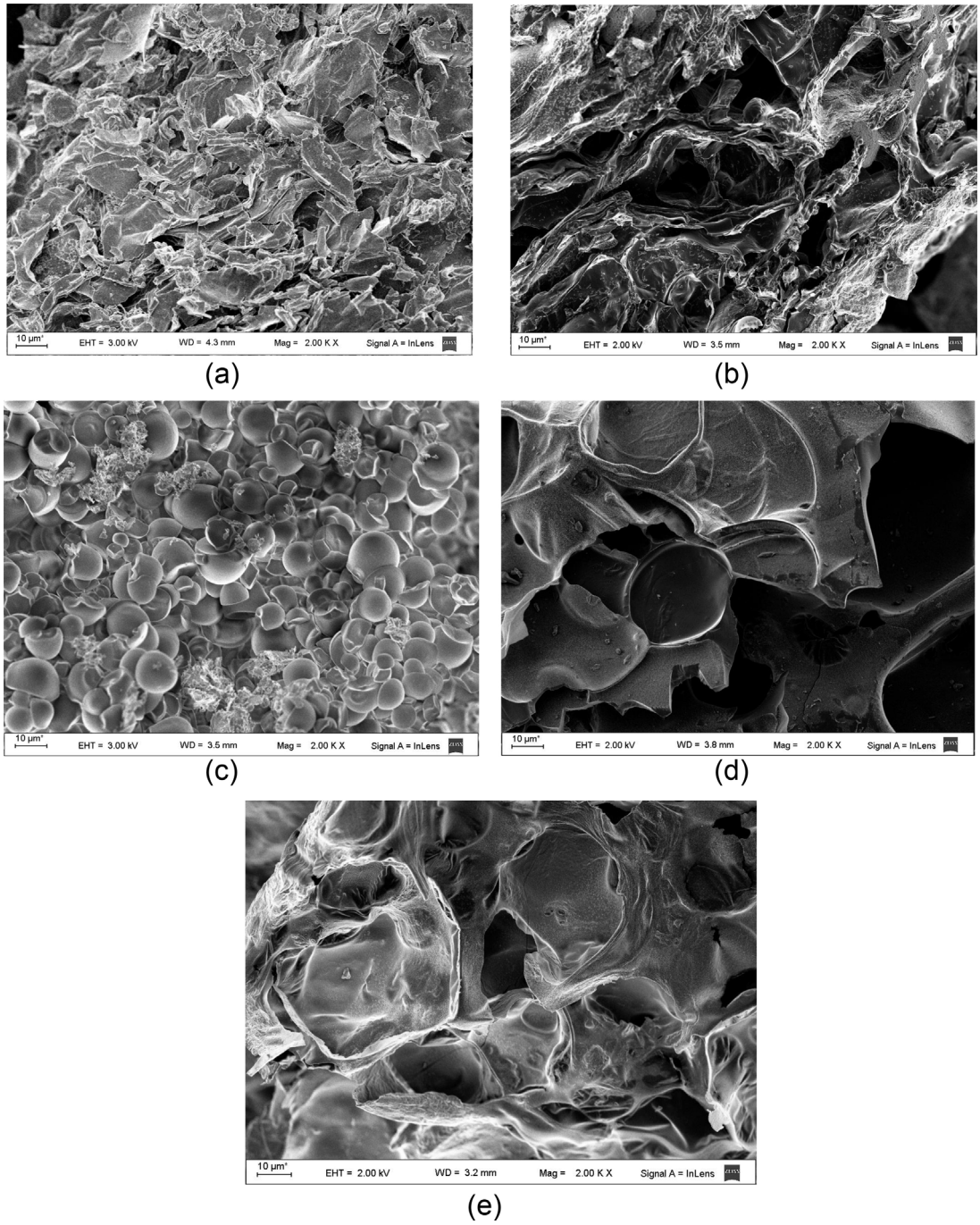

Fig. 4. SEM micrographs (2000×) of the raw materials and the bio-chars: (a) PS100; (b): PS100 bio-char; (c) ST; (d) ST bio-char; (e) PS50 bio-char.

with intermediate characteristics of the bio-chars discussed above (Fig. 4e) and, therefore, it would be expected that the change of the activation energy with the temperature ranges between those characterizing the pyrolysis of PS100 and ST.

Additionally, analyzing the values of the parameters of the distributed activation energy model it is seen that the standard deviation σ increased as the starch content decreased. The thermal degradation of cassava starch, which consists mainly of two polysaccharides formed by the same monomer, could take place through a less number of reactions than the peanut shells, composed by a more complex biopolymeric structure. Moreover, several minerals present in the shells could favor different scission reactions and complicate even more the pyrolysis mechanisms [37]. The intermediate values of σ for the pyrolysis of the mixtures suggest that the complexity of these thermal degradations is between those of the individual components.

3.3. Interactions between the starch and the lignocellulosic biopolymers

As discussed in the previous section, interactions between the cassava starch and the peanut shells could be inferred from the analysis of the DTG curves in Fig. 3a–c. Previously, the thermal degradation of the amylopectin and the amylose was also carried out in order to examine possible interactions between those two biopolymers that constitute the starch. Since no noticeable interactions were found, it is reasonable to hypothesize that the thermal degradation of a mixture of these two polysaccharides behaves as a

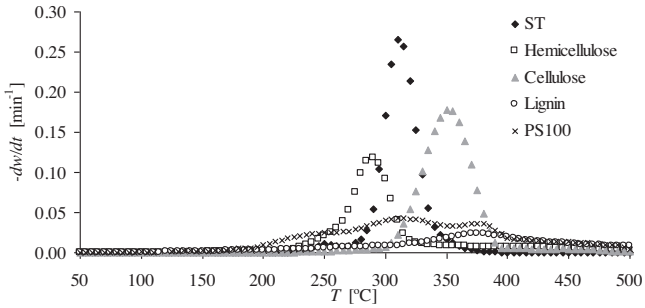

Fig. 5. DTG curves for the pyrolysis of cassava starch (ST) and the lignocellulosic biopolymers present in the peanut shells (hemicellulose, cellulose, and lignin). DTG curve of PS100 is included for comparison.

single component. Other authors reached the same conclusion [38]. For this reason, instead of investigating the interactions between these two biopolymers and those present in the peanut shells, only the interactions between starch as a whole and the lignocellulosic biopolymers were examined.

DTG curves of the pyrolysis of ST and the three investigated lignocellulosic biopolymers are comparatively shown in Fig. 5. Despite being composed by the same monomer, D-glucopyranose, it may be seen that the pyrolysis of the cassava starch and cellulose attained different maximum thermal degradation rates and the temperatures at which they occurred were also different. The cellulose, having its monomers linked by β-glycosidic bonds, forms linear chains of high polymerization degree. On the contrary, the starch monomers are linked by α-glycosidic bonds which allow branches or coils to occur, and thus, its crystallinity and polymerization degree are lower than those of the cellulose [39]. This could explain the higher resistance of cellulose to degrade thermically in comparison with that of the starch. In turn, hemicellulose, being a polymer made of different pentoses and hexoses, also has a lower polymerization degree than the cellulose and its decomposition starts at lower temperatures. On the other hand, lignin degrades over a wide range of temperatures and exhibits a considerable resistance to thermal decomposition due to its aromatic nature [29].

The copyrolysis of the binary mixtures of starch with hemicellulose, cellulose, and lignin in equal proportions are shown in Fig. 6a–c, respectively. The experimental data are compared with the calculated values (using a modification of Eq. (1) where the content of PS100 is replaced by the one corresponding to each lignocellulosic biopolymer) in order to analyze the existence of interdependence. Pyrolysis of the three binary mixtures showed a lower maximum degradation rate than the weighed average value calculated for the pyrolysis of the two components of the mixtures. These antagonistic effects agree with the ones shown in Fig. 3a–c.

As seen in Fig. 6a, the maximum rate of decomposition of the hemicellulose–starch mixture took place at a lower temperature than the one resulting from the predicted values. In the case of hemicellulose–cellulose mixtures, it has been pointed out that interactions could be caused by the earlier decomposition of the former which forms a liquid phase that covers the latter and inhibits its degradation [22]. A similar approach might also explain the pyrolytic behavior of hemicellulose–starch mixtures. In addition, Fig. 6b shows that, when pyrolyzed together, the temperature where the maximum degradation rate of starch occurred was not affected by the presence of cellulose. Nevertheless, the cellulose peak disappeared, possibly indicating that the starch addition increased the reactivity of cellulose and the experimental peak arose from the sum of both decompositions. Likewise from Fig. 6c, it could be inferred that the copyrolysis of starch and lignin constrained the decomposition of the former and promoted to some degree the reactivity of the latter.

As it can be inferred from Fig. 6b, the presence of the starch would promote the increase of the reactivity of the cellulose composing the peanut shells. Accordingly, the maximum reaction rate temperature shifted toward values near 310 °C, corresponding to the starch decomposition (Fig. 5). As cellulose is the most abundant biopolymer in the peanut shells (Table 1), this behavior would prevail over the effects of the starch on the hemicellulose or the lignin. These results could explain the similarity in the temperature at which the maximum reaction rate took place for the pyrolysis of PS100, ST and their mixtures (PS75, PS50 and PS25) (Fig. 2b). It is also important to mention that the interactions between the starch and the investigated biopolymers would be slightly different than those resulting from the mixtures of the starch with the ones constituting the peanut shells since the latter also contain mineral matter which could catalyze the thermal degradation. Alkaline and alkaline earth metals (AAEM) present in lignocellulosic biomasses reportedly shift the volatile emission peak during pyrolysis to lower temperatures [40].

3.4. Yields of the pyrolysis/copyrolysis products

Yields of the three kinds of the pyrolysis products for the thermal degradation of the individual components and their mixtures are presented in Fig. 7. It may be seen that a greater starch content in the mixture led to a lower yield of the generated bio-char. These results are in accordance with the trend observed for the influence of the components proportion of the mixtures on the residual weight fractions (w_∞) of the TGA curves shown in Fig. 2a.

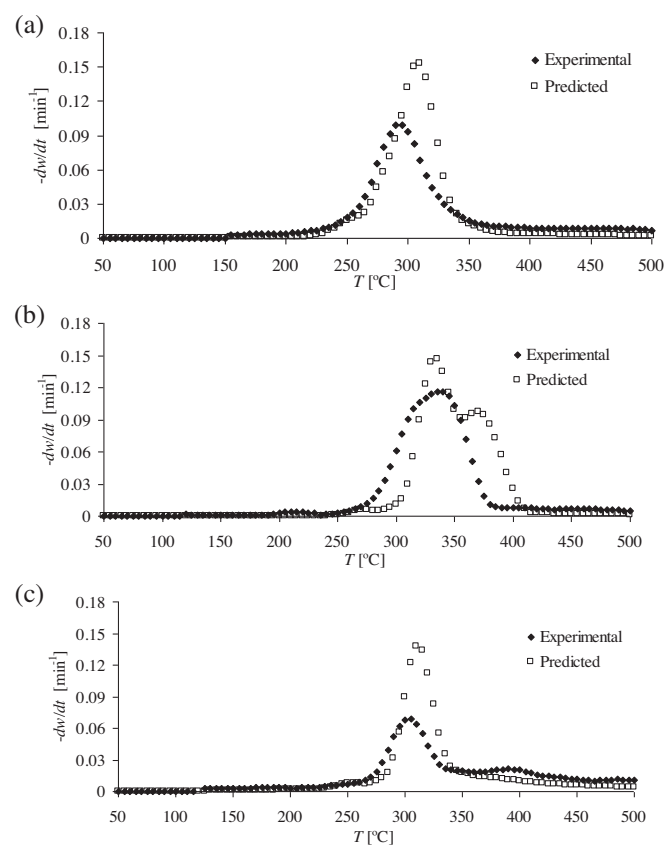

Fig. 6. Comparison between the experimental reaction rate and predicted values for the pyrolysis of mixtures of equal proportions of cassava starch and main lignocellulosic biopolymers present in the peanut shells: (a) hemicellulose–starch, (b) cellulose–starch, and (c) lignin–starch.

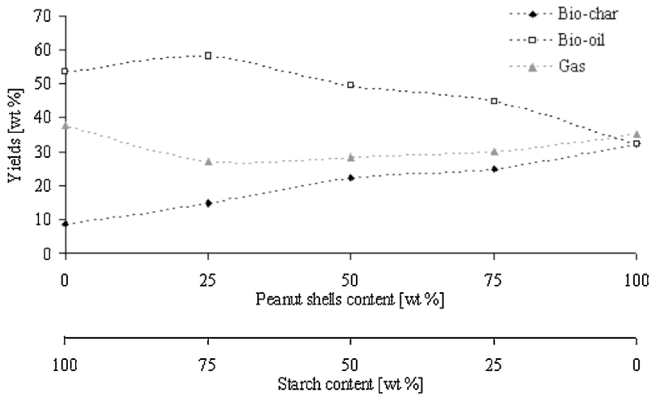

Fig. 7. Product yields for the pyrolysis of cassava starch (ST) and peanut shells (PS100) and for the copyrolysis of their mixtures (PS25, PS50 and PS75). Lines are included just to guide the eyes.

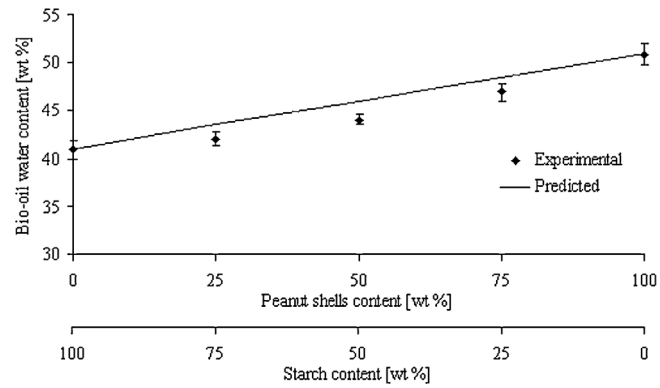

Fig. 8. Water content in the bio-oils from the pyrolysis of cassava starch (ST) and peanut shells (PS100) and from the copyrolysis of their mixtures (PS25, PS50 and PS75). Comparison between the experimental values and those predicted from the weighed average of the bio-oils' water content from the pyrolysis of the individual components.

The generation of the bio-oil and gas was strongly dependent on the composition of the sample. For mixtures with a high content of lignocellulosic biomass, the bio-oil yield increased and the gas generation slightly decreased as the starch content rose (Fig. **7**). On the other hand, for high starch content mixtures it seems that a maximum in bio-oil and a minimum in gas yield took place because the bio-oil generation from the pyrolysis of ST was lower than the one from pyrolysis of PS25. Other authors also reported a maximum in bio-oil generation for mixtures of biomass with an oxygenated biopolymer [41].

3.5. Properties of the pyrolysis/copyrolysis products

Table 3 shows the results of the elemental analysis and the pH of the bio-oils produced by the pyrolysis of the individual components and their mixtures. The liquids generated by the pyrolysis of the three binary mixtures had greater elemental carbon content than the individual components. As the elemental nitrogen content in the raw starch (Table 1) was very low (0.1 wt%), the presence of starch in the mixture, led to a bio-oil with less elemental nitrogen. Therefore, the NOx generation of these bio-oils obtained from pyrolysis of mixtures rich in starch would be insignificant [42]. pH values of the bio-oils were in the typical range of those reported in the literature [7]. These values were lowered as the content of starch in the mixture increased. As the starch has a lower degree of crystallinity and of polymerization than the cellulose, the thermal degradation of the former would favor scission reactions, thus, yielding greater amounts of low molecular weight compounds, such as formic and acetic acids, which in turn would reduce the pH of the bio-oil [43].

Table 3
Characterization of the bio-oils obtained from the pyrolysis of the peanut shells (PS100), the cassava starch (ST) and from the copyrolysis of their mixtures (PS25, PS50, PS75).

	PS100	PS75	PS50	PS25	ST
Ultimate analysis [wt%, dry basis][a]					
Carbon	49.3	57.9	53.5	50.0	49.5
Hydrogen	8.1	7.1	7.8	6.7	7.0
Nitrogen	2.9	1.9	1.7	0.3	0.1
Oxygen[b]	39.7	33.0	37.0	43.0	43.4
Bio-oil properties					
HHV [MJ/kg][a]	22.6	25.2	24.1	20.9	21.0
pH	3.1	2.9	2.9	2.8	2.7
Water content [wt%]	50.9	47.0	44.2	42.1	41.1

[a] Organic phase.
[b] Estimated by difference.

The water content of the different bio-oils is presented in Fig. 8. The predicted values were calculated from the weighed average of the bio-oils' water content from the pyrolysis of the individual components. The greater content of cassava starch in the mixtures subjected to pyrolysis resulted in bio-oils with lower water content. On one hand, and in spite of its higher moisture, the pyrolysis of ST yielded bio-oils with less water than the pyrolysis of PS100. As the peanut shells contain larger quantity of minerals, which could catalyze reactions that generate water, this would explain the less water generated in the pyrolysis of ST. On the other hand, since dehydration reactions could be correlated with bio-char yields, the smaller production of solids for the pyrolysis of ST also reinforces the found trend for the water content [29]. The relatively greater decrease in the water content of the bio-oils as higher the starch content in the sample could be due to synergistic effects [41]. This synergy could be caused by reactions between volatiles generated in the pyrolysis of each material or by reactions between volatiles and the pyrolyzed solids [44].

The FT-IR spectra of the bio-oils are presented in Fig. 9. Sharper peaks of aromatic ring vibrations (1500 cm^{-1} and 1595 cm^{-1}) [27] may be noticed for the bio-oils obtained from the pyrolysis of PS100 and PS75 mixtures. This would indicate a minor content of phenolic components, from lignin decomposition, in the bio-oils as the amount of starch in the mixture was raised. As the phe-

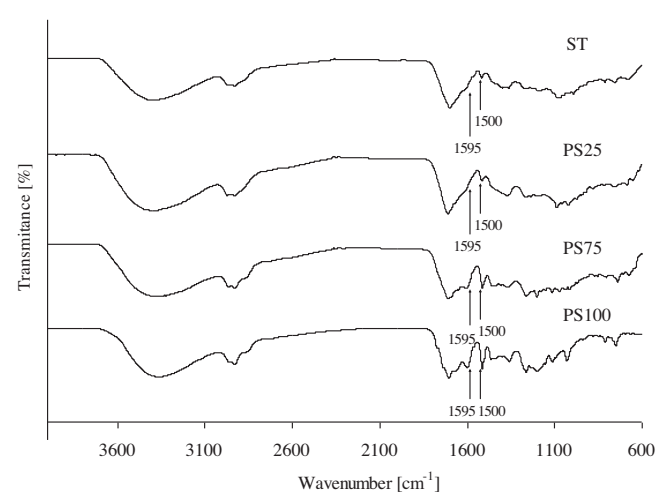

Fig. 9. Fourier-transform infrared (FT-IR) spectra for the bio-oils from the pyrolysis of cassava starch (ST) and peanut shells (PS100) and from the copyrolysis of their mixtures (PS25 and PS75).

Table 4
Chemical and textural characterization of the bio-char obtained from the pyrolysis of the peanut shells (PS100), the cassava starch (ST), and from the copyrolysis of their mixtures (PS25, PS50, PS75).

	PS100	PS75	PS50	PS25	ST
Ash [wt%, dry basis]	19.4	13.1	8.8	3.7	1.0
Ultimate analysis [wt%, dry and ash-free basis]					
Carbon	88.0	88.7	85.7	91.5	94.4
Hydrogen	2.3	2.3	3.0	1.9	2.1
Nitrogen	3.0	1.2	2.4	1.1	0.8
Oxygen[a]	6.7	7.8	8.9	5.6	2.7
HHV [MJ/kg]	32.2	32.6	32.3	33.5	35.1
Surface properties					
S_{BET} [m^2/g]	5	28	17	5	2
$V_T \times 10^3$ [cm^3/g]	3	14	8	5	2
r [nm]	1.2	1.0	0.9	2.1	2.0

[a] Estimated by difference.

nolic hydroxyl group is one of the most reactive functionalities of the bio-oil affecting its stability, the presence of starch in the mixtures subjected to pyrolysis would lead to a desirable reduction of phenolic compounds [45].

Bio-char properties are displayed in Table 4. As starch contains less ash (Table 1), the bio-char generated from the enriched-starch samples presented a small ash content, with the advantage of possible fouling reduction in case of further combustion. The pyrolysis of PS100 and ST samples resulted in non-porous materials. However, while PS100 pyrolysis generated a typical charcoal (Fig. 4b), the pyrolysis of ST led to a material more similar to a petcoke (Fig. 4d). Contrastingly, the bio-chars arising from the pyrolysis of PS75 and PS50 showed an increase of the BET area. Part of the pores, initially blocked by volatiles condensation, could have opened up during peanut shells pyrolysis. Partial gasification of the bio-char occasioned by H_2O or by CO_2 evolved from the starch could have been responsible of the explained porosity development [25], in turn resulting in higher S_{BET} values. In case of the PS25 bio-char, arisen from a mixture with a major proportion of starch, the petcoke film from starch pyrolysis could have covered all the pores resulting in a non-porous material.

The percent yields of the main gases of pyrolysis, calculated on the basis of kg of generated gas per kg of pyrolyzed sample, and the HHV of the gaseous mixtures for the pyrolysis/copyrolysis process are displayed in Table 5. The HHV of the gaseous products [MJ kg^{-1}] was calculated as the sum of the product of the moles of each gas generated per kg of gaseous mixture (G_i) and the heat of combustion of each gas [MJ mol^{-1}]:

$$\mathrm{HHV} = 0.802G_{CH_4} + 0.286G_{H_2} + 0.283G_{CO} \quad (9)$$

The results show that in all cases the majority gases were CO and CO_2. As seen, pyrolysis of mixtures with a greater content of starch than of peanut shells generated more CO_2 and less CO. The latter would be mainly produced by the secondary cracking of volatiles [46]. Since starch decomposition rate was high, an abrupt emission of gases could take place in the reactor, inducing an enhancement in gases production. Thus, the flow rate might be also enhanced by this brusque production of gases and, consequently, their residence time would fall. In this way, secondary reactions would be inhibited and, consequently, less CO would be generated. On the other hand, H_2 and CH_4 molar fractions decreased due to the addition of the starch. This could be attributed to the reduction of the lignin content in the sample as these two gases are mainly generated by the thermal degradation of this lignocellulosic biopolymer [46].

Table 5
Weight percent yields of the main pyrolysis gases and high heating value of the gaseous mixtures generated from the pyrolysis of the peanut shells (PS100), the cassava starch (ST), and from the copyrolysis of their mixtures (PS25, PS50, PS75).

	PS100	PS75	PS50	PS25	ST
CH_4 [wt%]	0.6	0.4	0.3	0.2	0.1
H_2 [wt%]	0.6	0.2	0.1	0.1	0.1
CO_2 [wt%]	14.2	15.4	18.5	15.8	24.5
CO [wt%]	16.0	10.8	8.2	9.0	9.2
HHV [MJ/kg]	8.8	5.8	3.9	4.5	3.3

4. Conclusions

Present results show that the copyrolysis of an agroindustrial lignocellulosic waste with cassava starch, a biopolymer copiously present in an agroprocessing refuse stream, may be an alternative to improve the yields and properties of the liquid products. Pyrolysis of the individual components and their mixtures was adequately described by the deactivation model and the distributed activation energy model. As the starch content in the mixture increased, the maximum degradation rate rose. The temperature at which this maximum degradation rate took place (310 °C) was not modified by the components proportion. In turn, the bio-oils generated in the fixed bed reactor had lower water content and higher elemental carbon percent than those individually generated by the pyrolysis of the peanut shells. The addition of the starch to the peanut shells led to a bio-char with less ash content, which could be more suitable for further combustion in steam boilers. The improved characteristics of the liquid and solid biofuels reinforce the importance of further studies in the area of the copyrolysis of lignocellulosic materials with waste stream biopolymers.

Acknowledgements

The authors gratefully acknowledge Agencia Nacional de Promoción Científica y Tecnológica (ANPCYT), Consejo Nacional de Investigaciones Científicas y Técnicas (CONICET) and Universidad de Buenos Aires (UBA) from Argentina, for financial support.

References

[1] H. Long, X. Li, H. Wang, J. Jia, Biomass resources and their bioenergy potential estimation: a review, Renew. Sustain. Energy Rev. 26 (2013) 344–352.
[2] P.R. Bonelli, G.V. Nunell, M.E. Fernandez, E.L. Buonomo, A.L. Cukierman, The potential applications of the bio-char derived from the pyrolysis of an agro-industrial waste. Effects of temperature and acid-pretreatment, Energy Sources Part A Recover. Util. Environ. Effects 34 (2012) 746–755.
[3] A. Adrados, A. Lopez-Urionabarrenechea, J. Solar, J. Requies, I. De Marco, J.F. Cambra, Upgrading of pyrolysis vapours from biomass carbonization, J. Anal. Appl. Pyrolysis 103 (2013) 293–299.
[4] S. Naik, V.V. Goud, P.K. Rout, K. Jacobson, A.K. Dalai, Characterization of Canadian biomass for alternative renewable biofuel, Renew. Energy 35 (2010) 1624–1631.
[5] A.L. Cukierman, G.V. Nunell, M.E. Fernandez, J. De Celis, M.R. Kim, L. Gurevich Messina, P.R. Bonelli, Thermochemical processing of wood from invasive arboreal species for sustainable bioenergy generation and activated carbons production, in: J.J. Blanco, A.T. Fernandes (Eds.), Invasive Species: Threats, Ecological Impact and Control Methods, Nova Publishers Inc., New York, 2012, pp. 1–45.
[6] L. Zhang, C. Xu, P. Champagne, Overview of recent advances in thermo-chemical conversion of biomass, Energy Convers. Manage. 51 (2010) 969–982.
[7] A.V. Bridgwater, Review of fast pyrolysis of biomass and product upgrading, Biomass Bioenergy 38 (2012) 68–94.
[8] J. Fan, T.N. Kalnes, M. Alward, J. Klinger, A. Sadehvandi, D.R. Shonnard, Life cycle assessment of electricity generation using fast pyrolysis bio-oil, Renew. Energy 36 (2011) 632–641.
[9] K. Jacobson, K.C. Maheria, A. Kumar Dalai, Bio-oil valorization: a review, Renew. Sustain. Energy Rev. 23 (2013) 91–106.
[10] F. Abnisa, W.M.A. Wan Daud, A review on co-pyrolysis of biomass: an optional technique to obtain a high-grade pyrolysis oil, Energy Convers. Manage. 87 (2014) 71–85.
[11] N. Thegarid, G. Fogassy, Y. Schuurman, C. Mirodatos, S. Stefanidis, E.F. Iliopoulou, K. Kalogiannis, A.A. Lappas, Second-generation biofuels by co-processing catalytic pyrolysis oil in FCC units, Appl. Catal. B Environ. 145 (2014) 161–166.

[12] A. Aho, T. Salmi, D. Yu Murzin, Catalytic pyrolysis of lignocellulosic biomass, in: K.S. Triantafyllidis, A.A. Lappas, M. Stöcker (Eds.), The Role of Catalysis for the Sustainable Production of Bio-Fuels and Bio-Chemicals, Elsevier Inc., London, 2013, pp. 137–159.
[13] T. Cornelissen, M. Jans, M. Stals, T. Kuppens, T. Thewys, G.K. Janssens, H. Pastijn, J. Yperman, G. Reggers, S. Schreurs, R. Carleer, Flash co-pyrolysis of biomass: the influence of biopolymers, J. Anal. Appl. Pyrolysis 85 (2009) 87–97.
[14] M.M. Wright, D.E. Daugaard, J.A. Satrio, R.C. Brown, Techno-economic analysis of biomass fast pyrolysis to transportation fuels, Fuel 89 (2010) S2–S10.
[15] E.D.M. Teixeira, A.A.S. Curvelo, A.C. Corrêa, J.M. Marconcini, G.M. Glenn, L.H.C. Mattoso, Properties of thermoplastic starch from cassava bagasse and cassava starch and their blends with poly (lactic acid), Ind. Crops Prod. 37 (2012) 61–68.
[16] FAOSTAT, Browse Data, Publication, Crops. Food and Agriculture Organization of the United Nations. Available from: http://faostat3fao.org/browse/Q/QC/E
[17] A.N. Jyothi, K. Sasikiran, B. Nambisan, C. Balagopalan, Optimisation of glutamic acid production from cassava starch factory residues using *Brevibacterium divaricatum*, Process Biochem. 40 (2005) 3576–3579.
[18] V. Muñoz, F. Ibañez, M.L. Tonelli, L. Valetti, M.S. Anzuay, A. Fabra, Phenotypic and phylogenetic characterization of native peanut *Bradyrhizobium* isolates obtained from Córdoba, Argentina, Syst. Appl. Microbiol. 34 (2011) 446–452.
[19] F. Duan, J.-P. Zhang, C.-S. Chyang, Y.-J. Wang, J. Tso, Combustion of crushed and pelletized peanut shells in a pilot-scale fluidized-bed combustor with flue gas recirculation, Fuel Process. Technol. 128 (2014) 28–35.
[20] P. Arromdee, V.I. Kuprianov, Combustion of peanut shells in a cone-shaped bubbling fluidized-bed combustor using alumina as the bed material, Appl. Energy 97 (2012) 470–482.
[21] M. Rhodes, Introduction to Particle Technology, second ed., John Wiley & Sons, Inc., Chichester, 2008.
[22] S. Wang, X. Guo, K. Wang, Z. Luo, Influence of the interaction of components on the pyrolysis behavior of biomass, J. Anal. Appl. Pyrolysis 91 (2011) 183–189.
[23] Q. Liu, S. Wang, Y. Zheng, Z. Luo, K. Cen, Mechanism study of wood lignin pyrolysis by using TG–FTIR analysis, J. Anal. Appl. Pyrolysis 82 (2008) 170–177.
[24] G.V. Nunell, M.E. Fernandez, P.R. Bonelli, A.L. Cukierman, Conversion of biomass from an invasive species into activated carbons for removal of nitrate from wastewater, Biomass Bioenergy 44 (2012) 87–95.
[25] K. Raveendran, A. Ganesh, Adsorption characteristics and of biomass-pyrolysis char, Fuel 77 (1998) 769–781.
[26] A. Rolland-Sabaté, T. Sánchez, A. Buléon, P. Colonna, B. Jaillais, H. Ceballos, D. Dufour, Structural characterization of novel cassava starches with low and high-amylose contents in comparison with other commercial sources, Food Hydrocolloids 27 (2012) 161–174.
[27] F. Xu, J. Yu, T. Tesso, F. Dowell, D. Wang, Qualitative and quantitative analysis of lignocellulosic biomass using infrared techniques: a mini-review, Appl. Energy 104 (2013) 801–809.
[28] T. Yuan, A. Tahmasebi, J. Yu, Comparative study on pyrolysis of lignocellulosic and algal biomass using a thermogravimetric and a fixed-bed reactor, Bioresour. Technol. 175 (2015) 333–341.
[29] F.-X. Collard, J. Blin, A review on pyrolysis of biomass constituents: mechanisms and composition of the products obtained from the conversion of cellulose, hemicelluloses and lignin, Renew. Sustain. Energy Rev. 38 (2014) 594–608.
[30] P.T. Marques, A.M.F. Lima, G. Bianco, J.B. Laurindo, R. Borsali, J.-F. Le Meins, V. Soldi, Thermal properties and stability of cassava starch films cross-linked with tetraethylene glycol diacrylate, Polym. Degrad. Stab. 91 (2006) 726–732.
[31] P.R. Bonelli, E.G. Cerrella, A.L. Cukierman, Slow pyrolysis of nutshells: characterization of derived chars and process kinetics, Energy Sources Recover. Util. Environ. Effects 30 (2003) 767–778.
[32] J.E. White, W.J. Catallo, B.L. Legendre, Biomass pyrolysis kinetics: a comparative critical review with relevant agricultural residue case studies, J. Anal. Appl. Pyrolysis 91 (2011) 1–33.
[33] J. Cai, R. Liu, New distributed activation energy model: numerical solution and application to pyrolysis kinetics of some types of biomass, Bioresour. Technol. 99 (2008) 2795–2799.
[34] A. García Barneto, J. Ariza Carmona, J.E. Martín Alfonso, R. Sánchez Serrano, Simulation of the thermogravimetry analysis of three non-wood pulps, Bioresour. Technol. 101 (2010) 3220–3229.
[35] X. Zhang, M. Xu, R. Sun, L. Sun, Study on biomass pyrolysis kinetics, J. Eng. Gas Turbines Power 128 (2004) 493–496.
[36] S. Balci, T. Dogu, H. Yucel, Pyrolysis kinetics of lignocellulosic materials, Ind. Eng. Chem. Res. 32 (1993) 2573–2579.
[37] P.R. Patwardhan, J.A. Satrio, R.C. Brown, B.H. Shanks, Influence of inorganic salts on the primary pyrolysis products of cellulose, Bioresour. Technol. 101 (2010) 4646–4655.
[38] X. Liu, L. Yu, H. Liu, L. Chen, L. Li, Thermal decomposition of corn starch with different amylose/amylopectin ratios in open and sealed systems, Cereal Chem. 86 (2009) 383–385.
[39] T. Lin, E. Goos, U. Riedel, A sectional approach for biomass: modelling the pyrolysis of cellulose, Fuel Process. Technol. 115 (2013) 246–253.
[40] L. Jiang, S. Hu, L. Sun, S. Su, K. Xu, L. He, J. Xiang, Influence of different demineralization treatments on physicochemical structure and thermal degradation of biomass, Bioresour. Technol. 146 (2013) 254–260.
[41] T. Cornelissen, J. Yperman, G. Reggers, S. Schreurs, R. Carleer, Flash co-pyrolysis of biomass with polylactic acid. Part 1: influence on bio-oil yield and heating value, Fuel 87 (2008) 1031–1041.
[42] J.-P. Cao, X.-Y. Zhao, K. Morishita, X.-Y. Wei, T. Takarada, Fractionation and identification of organic nitrogen species from bio-oil produced by fast pyrolysis of sewage sludge, Bioresour. Technol. 101 (2010) 7648–7652.
[43] P.R. Patwardhan, J.A. Satrio, R.C. Brown, B.H. Shanks, Product distribution from fast pyrolysis of glucose-based carbohydrates, J. Anal. Appl. Pyrolysis 86 (2009) 323–330.
[44] T. Cornelissen, M. Jans, J. Yperman, G. Reggers, S. Schreurs, R. Carleer, Flash co-pyrolysis of biomass with polyhydroxybutyrate: part 1. Influence on bio-oil yield, water content, heating value and the production of chemicals, Fuel 87 (2008) 2523–2532.
[45] T.-S. Kim, J.-Y. Kim, K.-H. Kim, S. Lee, D. Choi, I.-G. Choi, J.W. Choi, The effect of storage duration on bio-oil properties, J. Anal. Appl. Pyrolysis 95 (2012) 118–125.
[46] H. Yang, R. Yan, H. Chen, D.H. Lee, C. Zheng, Characteristics of hemicellulose, cellulose and lignin pyrolysis, Fuel 86 (2007) 1781–1788.